

## 2.4 NEW ADVANCES IN *IN VIVO* SMALL ANIMAL IMAGING

**F. Pain and P. Laniece**  
**Institut de Physique Nucleaire, Orsay, France**

The emergence of new animal models that mimic human disorders (neurodegenerative diseases, tumour growth, neuropsychiatric disorders) have enabled new fundamental and therapeutical approaches of these diseases. Mice, rats or guinea pigs have become progressively ubiquitous participants in most areas of molecular biology, toxicology and drug discovery research. Well-characterized models have been thus developed for a wide range of diseases to offer the possibility of studying their fundamental mechanisms as well as to test potential drugs. The mouse, in particular, has become a key animal model system for the study of development and human disease [1-4]. It offers the possibility to manipulate its genome and produce accurate models of many human disorders resulting in significant progress in the understanding of human diseases. In neurobiology, the possibility to mimic neurodegenerative diseases with rat models has permitted the development and the assessment of new therapeutic strategies based on genetic therapy or cell grafts [5-8].

The increasing number of studies performed on animal models has stimulated the development of new imaging tools adapted to the particular constraints of *in vivo* studies in small animals. *Ex vivo* experiments such as autoradiography have indeed showed their limitations when subjected to longitudinal analyses required in the studies involving animal models. They are expensive, time consuming, and barely precise due to the important inter-individual physiological variation. Extension of modern biomedical imaging techniques to the small animal has presented therefore some interesting challenge and opportunities. This has led to the emergence of dedicated systems including radiotomography and magnetic resonance imaging technologies. The aim of this article is to review briefly these systems and to illustrate their performance in biological contexts.

### *Radioimaging systems.*

By their principle, radioimaging techniques do not deliver anatomical images. Associated with specific radiotracers, they furnish metabolic data of different orders from which it can be cited as examples the functional and oncological imaging with  $^{18}\text{F}$ -FDG [9-11], the evaluation of new radiopharmaceutical for diagnostic efficiency [12], the evaluation of new receptor ligand [13], or more recently the reporter gene expression imaging [14]. Since 1990, different instrumental approaches based on Single Photon Emission Computed Tomography (SPECT) and Positron Emission Tomography (PET) systems have been investigated. The use of geometry with best compactness and the development of algorithm with best accuracy has led to the conception of tomographs with a spatial resolution of the order of 2 mm [15, 16]. In practice, the fundamental spatial resolution of PET systems is limited by the average distance that the emitted positron travels before it annihilates and by the residual momentum of the electron-positron pair at annihilation which results in gamma rays being emitted with a small deviation from the assumed  $180^\circ$ . In the case of SPECT cameras, the spatial resolution depends on the geometry of the collimation system. If, theoretically, it should be possible to conceive camera yielding submillimetric spatial resolution using collimators with holes of very small diameter, the very low efficiency which should result of such a geometry would impose non realistic acquisition time and to strong injected doses. This condition has led to the conception of camera SPECT which can usually only be employed for visualizing static tracer distributions whereas their planar imaging variants can analyze rapidly changing activity distributions albeit with less accuracy. Among

the numerous PET scanners which have been dedicated to small animals, some systems have already furnished some promising results and are now commercially available.



Figure 1:  $^{18}\text{F}$ -FDG rat images obtained with MicroPET, the animal PET developed at UCLA. Top: coronal cross-sections through the whole body. Middle: transverse sections through the level of heart. Bottom: coronal brain sections. Acquisition time varied from 90 minutes (top) to 40 minutes (others). (from [17])

As an example, figures 1 and 2 present images obtained from animal PET systems showing for once a few example of biological applications performed with  $^{18}\text{F}$ -FDG [17] and for other the specific problem of resolution illustrated through the binding of a radiotracer in a specific region of the central nervous system called striatum. One can observe on figure 2.1 the perfect distinction of the both lobes of striatum obtained in primate and rat, discrimination which became more ambiguous in mouse since the distance between both lobes is near than the intrinsic resolution of the tomograph [18].

Figure 2.1: PET images of horizontal (top) and coronal (bottom) brain sections of primate, rat and mouse performed with MicroPET, the animal PET developed at UCLA. Black areas correspond to striatum revealed after the injection of  $[^{11}\text{C}]\text{-CFT}$ , a tracer of the dopaminergic system. Image time: 50 minutes; injected doses: 5 mCi (primate), 1 mCi (rat); 180  $\mu\text{Ci}$  (mouse). (from [18]).

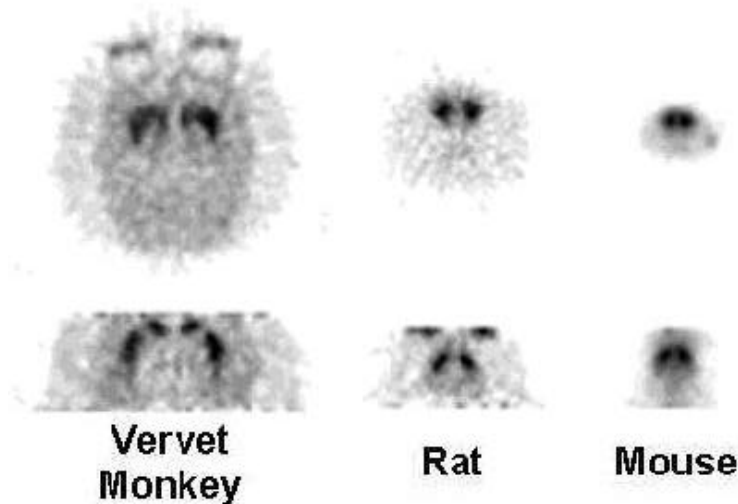


Figure 2.2 shows that alternate PET systems can offer optimized images leading to a perfect distinction of the structures in mice [19]. Nevertheless, this can be done only by an important increase of time acquisition (20 minutes in

this example) what prevents in particular the possibility to have dynamic information on the binding kinetic of the tracer. In addition to SPECT and PET systems, other tomographs have been developed specifically for small animal imaging based on principles different from current SPECT and PET.

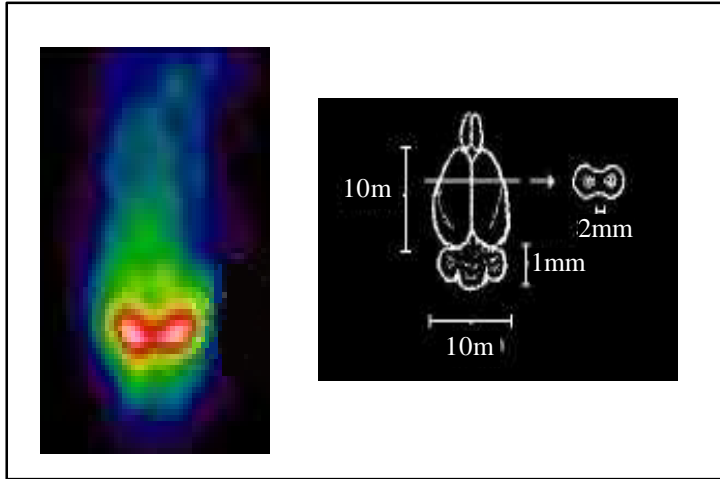
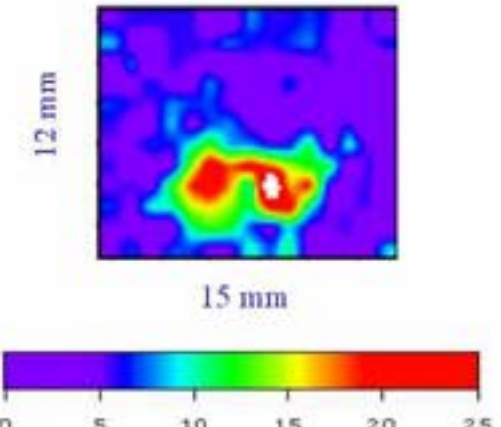


Figure 2.2: PET image of mouse coronal brain section obtained with PET HIDAC, the animal PET developed by Oxford positron systems (UK). Striatum is as well revealed after injection of  $[^{11}\text{C}]\text{-CFT}$ . Image time: 20 minutes; injected dose: 67  $\mu\text{Ci}$ . (from [19])

Figure 3 shows accumulation of  $^{123}\text{I}$  in a rat thyroid obtained with TOHR. The 1.4 mm resolution allows to visualize not only both lobes of the structure but also the isthmus connecting both lobes.

Figure 3: Image of a thyroid rat section obtained with TOHR after the injection of free  $^{123}\text{I}$ . Image time: 30 minutes; injected dose: 60  $\mu\text{Ci}$ .

This is in particular the case of TOHR, a tomograph developed at University of Orsay (France) with high resolution and small field of view [20]. It is a  $\gamma$  or X-ray counter composed of a large solid angle, focusing collimator coupled with a set of radiation detectors. Here, the backprojection is avoided by directly measuring the activity concentration in a small volume assumed as a voxel of the image, and the tomographic image is accumulated by moving the sample relative to the detector to scan the volume of interest.



*Magnetic resonance imaging systems*

One of the major advantages of the magnetic resonance imaging (MRI) is that the technique can deliver both anatomical and metabolic images. Since the

technique is based on the detection of nucleus having some specific magnetic properties, these nuclei can be from exogenous source (injection of paramagnetic tracer) or from endogenous source (detection of signal issued from protons  $^1\text{H}$ , or from nuclei  $^{13}\text{C}$ ,  $^{19}\text{F}$ ,  $^{31}\text{P}$ , or even from an endogenous paramagnetic molecule: the deoxyhemoglobin).

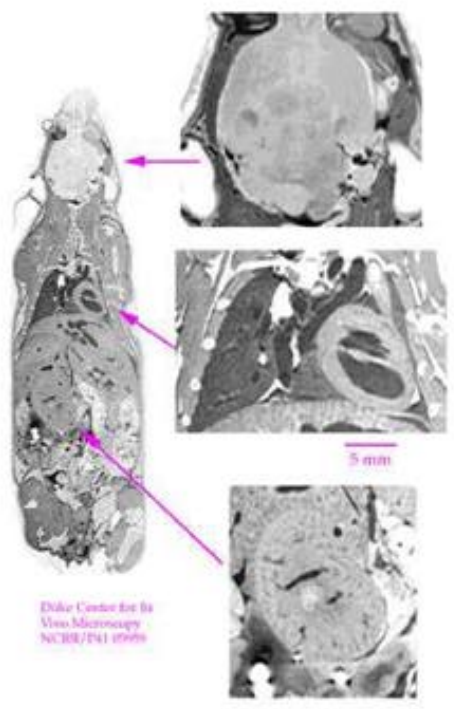
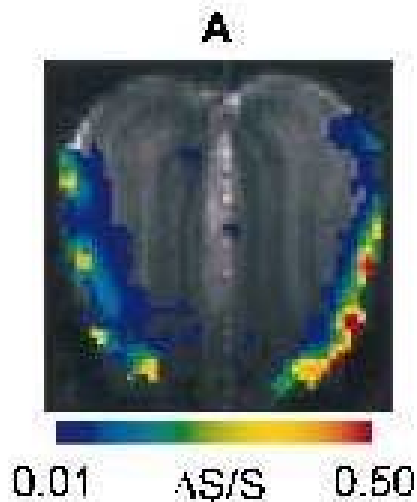


Figure 4: MRI<sub>a</sub> image of the whole body of a mouse with isotropic resolution of  $100 \times 100 \times 100 \mu\text{m}$  acquired at the Duke center for in vivo microscopy.

As for SPECT systems, extension of MRI to small animal is based on a trade-off between resolution and sensitivity. Indeed, the magnetic field necessary to obtain a resonance (and thus a relaxation of the magnetic nucleus) is applied as a gradient to combine the location information. The spatial resolution is thus fixed by this gradient whereas the sensitivity of the system, ie the intensity of measured signals, depends on both the magnetic field intensity and the measured volume fixed by the resolution and

the acquisition time. The increase of the spatial resolution is therefore based on the choice of a suitable gradient to preserve detectable signals. This can easily be reached by increasing the intensity of the magnetic field, the acquisition time, or the region of interest, conditions difficult to adapt on human but not on rodent. According to these constraints, the parametric conditions are different according to the type of MRI expected. The anatomic MRI (MRI<sub>a</sub>) which is based on the detection of relatively high signals is obtained by using long acquisition times and a low magnetic fields (around 1.5 to 2 T). This allows to obtain images with a spatial resolution yielding 100 μm (see figure 4, [21]) particularly well suited to the rodent tissue dimensions [22]. This is for instance very potential to analyze the phenotype changes of genetically modified mice.



The functional MRI (MRI<sub>f</sub>) which is based on the detection of low detectable signals is obtained by using high magnetic fields (from 3 to 10 T) and a trade-off between the probed volume dimension and the acquisition time [23]. To adjust the low sensitivity of the method, it is indeed necessary to realize measurements on large volumes since the dynamic nature of the physiologic information is not compatible with long time acquisition [24]. Techniques using injection of exogenous molecules as enhancer have been recently proposed to increase the sensitivity of the method [25, 26]. Two examples are shown on figures 5 and 6 where one can appreciate in particular the possibility to superimpose directly the dynamic image on the anatomical image from the same animal [26, 27].

Figure 5: Image of a frontal brain section of a rat acquired with a 7 T magnet (from [27]).

In color: MRI<sub>f</sub> of the olfactory bulb after an olfactory stimulation obtained with a 220 μm x 220 μm x 1 mm spatial resolution et 36 s temporal resolution. In grey: correspondent high resolution MRI<sub>a</sub>.

Figure 6: frontal rat brain distribution of a cerebral blood flow increase after the injection of 1 mg/kg cocaine revealed by MRI<sub>f</sub>. Images were realized with a 2 T magnet after the injection of a paramagnetic enhancer and superimposed with MRI<sub>a</sub> images. Spatial resolution: 0.6 mm<sup>2</sup>; temporal resolution: 10 s. (from [26]).

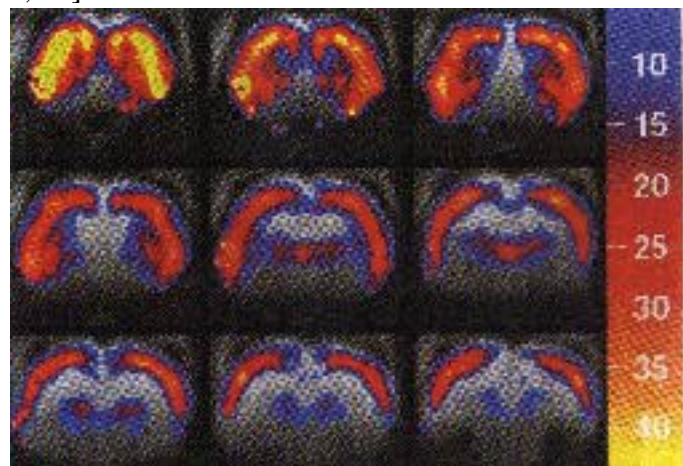


Figure 6: frontal rat brain distribution of a cerebral blood flow increase after the injection of 1 mg/kg cocaine revealed by MRI<sub>f</sub>. Images were realized with a 2 T magnet after the injection of a paramagnetic enhancer and superimposed with MRI<sub>a</sub> images. Spatial resolution: 0.6 mm<sup>2</sup>; temporal resolution: 10 s. (from [26]).

In conclusion, one of the most promising areas of application for imaging in the biomedical sciences is the study of small animal models. Radioimaging and MRI systems as well as computed tomography, ultrasound systems, echography and optical imaging are now available for rodent. Biomedical programs are on progress worldwilde to use those potential tools on animal models. At present, focus is on the possibility to obtain simultaneously complementary measurements on the same animal by combining the techniques [28-30]. This will offer tools able to furnish both high spatial and temporal resolution anatomical and dynamical images of the small animal. The ability of these powerful tools will be enhanced by other improvements which are as well under development and which concern both the complete monitoring of the animal during experiments (control of physiological parameters) and the possibility to perform studies on awake and freely moving animals [31].

## REFERENCES

- [1] Poltorak A, He X, Smirnova I, Liu MY, Huffel CV, Du X, Birdwell D, Alejos E, Silva M, Galanos C, Freudenberg M, Ricciardi-Castagnoli P, Layton B, Beutler B. Defective LPS signaling in C3H/HeJ and C57BL/10ScCr mice: mutations in Tlr4 gene. *Science* Dec 282, 1998, 2085-8
- [2] Giros B, Jaber M, Jones SR, Wightman RM, Caron MG. Hyperlocomotion and indifference to cocaine and amphetamine in mice lacking the dopamine transporter. *Nature* Feb 379, 1996, 606-12
- [3] Defective inflammatory response in interleukin 6-deficient mice. Fattori E, Cappelletti M, Costa P, Sellitto C, Cantoni L, Carelli M, Faggioni R, Fantuzzi G, Ghezzi P, Poli V *J Exp Med* Oct 180, 1994, 1243-50
- [4] Gu L, Tseng S, Horner RM, Tam C, Loda M, Rollins BJ. Control of TH2 polarization by the chemokine monocyte chemoattractant protein-1. *Nature* Mar 404, 2000, 407-11
- [5] E. Brouillet, M. C. Guyot, V. Mittoux, S. Altairac, F. Condé, S. Palfi, and P. Hantraye, Partial inhibition of brain succinate dehydrogenase by 3-nitropropionic acid is sufficient to initiate striatal degeneration in rat. *J Neurochem.*, vol. 70, 1998, 794-805.
- [6] P. Hantraye. Modeling dopamine system dysfunction in experimental animals. *Nucl. Med. Biol.*, vol. 25, 1998, 721-728,.
- [7] E. Brouillet, F. Condé, M. F. Beal, and P. Hantraye. Replicating Huntington's disease phenotype in experimental animals. *Progress in Neurobiol.*, 1999, *In press*,
- [8] Corti O, Sanchez\_Capelo A, Colin P, Hanoun N, Hamon M, Mallet J. Long-term doxycycline-controlled expression of human tyrosine hydroxylase after direct adenovirus-mediated gene transfer to a rat model of Parkinson's disease. *Proc Natl Acad Sci U S A* Oct 12 96:21, 1999, 12120-5
- [9] Kornblum H, Araujo D, Annala A, Tatsukawa K, Phelps M, Cherry S. In vivo imaging of neuronal activation and plasticity in the rat brain by high resolution positron emission tomography (microPET). *Nat. Biotech.*, 18, 2000, 655-660.
- [10] Rigo P, Paulus P, Kaschten BJ, Hustinx R, Bury T, Jerusalem G, Benoit T, Foidart-willems J. Oncological applications of positron emission tomography with fluorine-18 fluorodeoxyglucose. *Eur J Nucl Med*, 23, 1996, 1641-1674.
- [11] Wu AM, Yazaki P, Tsai S, Nguyen K, Anderson A, McCarthy D, Welch M, Shively J, Williams L, Raubitschek A, Wong J, Toyokuni T, Phelps M, and Gambhir S. High-resolution microPET imaging of carcino-embryonic antigen-positive xenografts by using a copper-64-labeled engineered antibody fragment. *Proc Natl Acad Sci U S A*, July 18 97:15, 2000, 8495-8500.

- [12] Guilloteau D, Emond P, Baulieu JL, Garreau L, Frangin Y, Pourcelot L, Mauclaire L, Besnard JC and Chalon S. Exploration of the dopamine transporter: In vitro and In vivo characterisation of a high-affinity and high-specificity iodinated tropane derivative (E)-N-(3-iodoprop-2-enyl)-2 $\beta$ -carbomethoxy-3 $\beta$ -(4'-methylphenyl)nortropane (PE2I). *Nucl Med Biol.*, 25, 1998, 331-337.
- [13] Hume SP. Quantification of carbon-11-labeled raclopride in rat striatum using PET. *Synapse*, 12, 1992, 47-54.
- [14] Ogawa O, Umegaki H, Ishiwata K, Asai Y, Ikari H, Oda K, Toyama H, Ingram DK, Roth GS, Iguchi A, Senda M. In vivo imaging of adenovirus-mediated over expression of dopamine D2 receptors in rat striatum by positron emission tomography. *Neuroreport*, 11, 2000, 743-748.
- [15] Hume SP, Gunn RN, Jones T. Pharmacological constraints associated with positron emission tomographic scanning of small laboratory animals. *Eur J Nucl Med*, 25:2, 1998, 173-6.
- [16] Weber DA, Ivanovic M, Franceschi D, Strand SE, Erlansson K, Franceschi M, Atkins HL, Coderre JA, Susskind H, Button T, Ljunggren K. Pinhole SPECT : an approach to in vivo high resolution SPECT imaging in small laboratory animals. *J. Nucl Med*, 35, 1994, 342-348.
- [17] Cherry S. High resolution Pet instrumentation for small animal imaging. Proceedings of "in vivo microscopy: technologies and applications" a workshop for small animal imaging, march 18 & 19, 1999, Gaithersburg, MD, pp 8-10.
- [18] Chatziionannou AF, Cherry SR, Shao Y, Silverman RW, Meadors K, Farquhar TH, Pedarsani M, Phelps ME. Performance evaluation of microPET: a high resolution lutetium oxyorthosilicate PET scanner for animal imaging. *J. Nucl. Med*, 40 (7), 1999, 1164-1175.
- [19] Jeavons AP, Chandler RA, Dettmar CAR. A 3D HIDAC-PET Camera with Sub-millimetre Resolution for imaging Small Animals. *IEEE Trans Nucl Sci*, 46, 1999, 468-473.
- [20] Valda-Ochoa A, Ploux L, Mastrippolito R, Charon Y, Lanière P, Pinot L, Valentin L. An original emission tomograph for in vivo brain imaging of small Animals. *IEEE Trans Nucl Sci*, 44, 1997, 1533-1537.
- [21] Johnson GA. MR Microscopy. Proceedings of "in vivo microscopy: technologies and applications" a workshop for small animal imaging, march 18 & 19, 1999, Gaithersburg, MD, pp 4-6.
- [22] Bittoun J, Gonord P, Ruaud JP, Kan S, Sauzade M; Principles of magnetic resonance imaging and microscopy. *J. Trace and Microprobe Techniques*, 13(3), 1995, 267-283.
- [23] Ogawa S, Lee TM, Nayak AS, Glynn P. Oxygenation sensitive contrast in magnetic resonance image on rodent brain at high magnetic field. *Magn Reson Med*, 14, 1990, 68-78.
- [24] Menon RS, Kim SG. Spatial and temporal limits in cognitive neuroimaging with fMRI. *Trends in Cognitive Sciences*, 3, 1999, 207-216.

- [25] van Bruggen N, Busch E, Palmer JT, Williams SP, de Crespigny AJ. High resolution functional magnetic resonance imaging of the rat brain: mapping changes in cerebral blood volume using iron oxide contrast media. *J Cereb Blood Flow Metab*, 18, 1998, 1178-1183.
- [26] Marota JJA, Mandeville JB, Weisskoff RM, Moskowitz MA, Rosen BR, Kosofsky BE. Cocaine Activation discriminates Dopaminergic projections by temporal Response: an fMRI study in Rat. *NeuroImage*, 11, 2000, 13-23.
- [27] Yang X, Rneken R, Hyder F, Siddeek M, Greer CA, sheperd GM, Shulman RG. Dynamic mapping at the laminar level of odor-elicited responses in rat olfactory bulb by functional MRI. *Proc Natl Acad Sci U S A*, 95, 1998, 7715-7720.
- [28] Nandor L, Hai MT. Cellular electrophysiological changes in the hippocampus of freely behaving rats during local microdialysis with epileptogenic concentration of N-methyl-d-aspartate. *Brain Research Bulletin*, 51, 2000, 233-240.
- [29] Slates RB, Farahani K, Shao Y, Marsden PK, Taylor J, Summers PE, William S, Beech J, Cherry SR. A study of artefacts in simultaneous PET and MR imaging using a prototype MR compatible scanner. *Phys Med Biol*, 44, 1999, 2015-2027.
- [30] Endres CJ. Kinetic Modeling of <sup>11</sup>C-raclopride: combined PET-microdialysis studies. *J Cereb Blood Flow Metab*, 17, 1997,
- [31] Pain F., Laniece P., Matrippolito R., Charon Y., Comar D., Leviel V., Pujol J.F., Valentin L.. SIC, an intracerebral radiosensitive probe for *in vivo* neuropharmacology investigations in awake small laboratory animals: theoretical considerations and physical characteristics. *IEEE Trans. Nucl. Sci.* 47, n°1, 2000, 25-32.